RASPT2 study of the valence excited states of an iron–porphyrin–carbonyl model complex

Nadia Ben Amor, Marie-Catherine Heitz

RASPT2 study of the valence excited states of an iron-porphyrin-carbonyl model complex

Nadia Ben Amor*, Marie-Catherine Heitz*

Abstract

Multireference wavefunction calculations of the singlet valence excited states of an iron-porphyrin-pyrazine-carbonyl complex up to the Soret band (about 3 eV) are presented. This complex is chosen to be a model for the active site of carboxy-hemoglobin/myoglobin. The investigations are performed at the Restricted Active Space Second Order Perturbation (RASPT2) level involving an extended active space on the porphyrin ligand in addition to the active orbitals needed for the description of the metal-ligand interactions. Metal-to-Ligand-Charge-Transfer states $d \rightarrow \pi^*$ and some Metal-Centered $d \rightarrow d$ transitions are found in the lowest part of the spectrum, below the first $\pi \rightarrow \pi^*$ intraporphyrin transitions (Q band). Doubly excited states involving simultaneous intraporphyrin and metal centered excitations are found in the vicinity of the second set of intraporphyrin transitions (the so-called Soret band). The effect of the extension of the active space on the porphyrin ligand beyond the Gouterman's orbitals set is investigated together with the effect of inclusion of the Ionization Potential Electronic Affinity (IPEA) shift in the RASPT2 treatment.

Keywords: RASPT2, IPEA, Metalloporphyrin, Iron, Excited states

*Laboratoire de Chimie et Physique Quantiques, Université de Toulouse et CNRS, UT3 - Paul Sabatier, 118, Route de Narbonne, F-31062 Toulouse Cedex - France

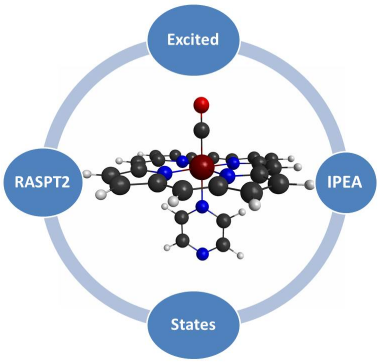

The singlet valence excited states of an iron-porphyrin-pyrazine-carbonyl complex up to the Soret band (about 3 eV) were calculated at the Restricted Active Space Second Order Perturbation (RASPT2) level involving an extended active space. This complex is chosen to be a model for the active site of carboxy-hemoglobin/myoglobin. The effect of inclusion of the Ionization Potential Electronic Affinity (IPEA) shift in the RASPT2 treatment was investigated.

INTRODUCTION

Metalloporphyrins are playing an important role in fundamental processes in biological functions like oxygen transport and activation[1] or in biomimetic catalysis[2,3].

They can also be photoactivated through the excitation of the strongly absorbing porphyrin ring in the visible or ultra-violet region. The presence of an extended π-conjugated chromophore and of a metallic center leads to a variety of dynamical processes such as charge transfer, dissociation of axial ligands, internal conversion and intersystem crossings. These excited state processes can be studied in a biological environment[4,5], in the condensed[6] or gas[7] phases.

In this work, we focus on an iron-porphyrin complex with two axial ligands, namely a carbonyl and a pyrazine (pz) ligand. This FeP(pz)CO complex is considered as a model for the active site of carboxyhemoglobin or carboxymyoglobin. Hemoglobin and myoglobin are well known for performing the transport and the storage of O_2, but they can also bind other small molecules such as CO or NO. In the case of CO, the interaction with IR-light can be used experimentally to probe the ligand transfer inside the protein[8–10] or to perform vibrational ladder climbing[11] to populate high vibrational excited states. From the theoretical side, various molecular processes have been studied: photodissociation mechanism of CO[12–14], dynamics of spin transitions[14] and vibrational dynamics[15,16]. In this paper, we present Restricted and Complete Active Space Second Order Perturbation RASPT2[17] and CASPT2[18] calculations of the valence singlet excited states (until ≈ 3 eV) of the FeP(pz)CO complex. Compared to the standard model used for representing the active site of either hemoglobin or myoglobin, we replace the imidazole ($C_3H_4N_2$) group by a pyrazine ($C_4H_4N_2$) group, leading to a complex of C_{2v} symmetry. This reduces the number of states in each irreducible representation, making the calculations more tractable. Indeed, iron-porphyrins are so-called irregular porphyrins where the partially filled d-shell contributes significantly to the excited state spectrum through excitations from or to metallic orbitals. Thus, the challenge is the balanced description of the two subsystems (the porphyrin π system and the 3d-shell of the iron) to describe in a consistent way the various excitations of the valence

spectrum: Metal-Centered (MC) and Metal-to-Ligand-Charge-Transfer (MLCT) transitions, intra-porphyrin excitations and mixed double excitations. Excited states involving excitations to the pyrazine ligand are not investigated in the present work. The metallic site of carboxy-hemoglobin/myoglobin is experimentally assigned to a diamagnetic ground state (see for instance Refs[19] and[20]). This can be rationalized on the basis of the strong ligand field of CO[21]. We thus focus on singlet excited states .

Multireference perturbative methods are commonly used for calculations of excited states (see recent review in ref[22]). The introduction of dynamical correlation thanks to methods like CASPT2 in 1990 and then RASPT2 in 2008 represented an important step towards the study of excited states of large systems. In 2004, a modification of the zeroth-order Hamiltonian in the CASPT2 and then in the RASPT2 methods was proposed to compensate an unbalanced treatment of closed and open shells[23]. The so-called Ionization Potential Electronic Affinity (IPEA) shift, a single parameter whose numerical value (0.25 a.u.) was selected from benchmark calculations, was supposed to be systematically used from then on[23]. More recently, discussions about the use of IPEA, and its specific numerical value, have appeared in the literature, concerning organic systems in general[24,25], iron compounds[26,27] and free-based and regular porphyrins[28] in particular. In the present work, calculations with and without the use of the IPEA shift are compared. The second aspect we wish to highlight in this work is the composition of the active space on the porphyrin ligand. Gouterman, in the 1960s, rationalized the absorption spectra of porphyrins on the basis of one-electron transitions between the four frontier orbitals of the conjugated cycle[29,30]. In our previous study[31], the active space on the porphyrin was restricted to this so-called Gouterman's set. Taking also into account all the orbitals required for the description of the iron and the metal-ligand interactions according to standard rules[32–34], we reported CASPT2 calculations based on a 14 electrons in 14 active orbitals space[31]. In the present work, we present RASPT2 calculations including an extended active space on the porphyrin, beyond the four Gouterman's frontier orbitals and we discuss the effect of the IPEA shift in connection with the enlargement of the active space.

COMPUTATIONAL METHODS

Computational details

The calculations were performed at the same geometry as the previous CASPT2 study[31]. This structure of C_{2v} symmetry is displayed in Figure 1 (plotted with MacMolPlt[35]). The N(pyrazine)-Fe-C-O chain is chosen to lie along the z-axis while the Fe-N(porphyrin) bonds are bisectors of the xz and yz planes. The coordinates can be found in the Supplementary Material of Ref[31]. As expected considering the strong ligand field of CO and the d^6 configuration of the iron, the electronic ground state of the complex is a closed-shell singlet. The results of the geometry optimizations of other spin states based on DFT calculations are summarized in the Supplementary Material.

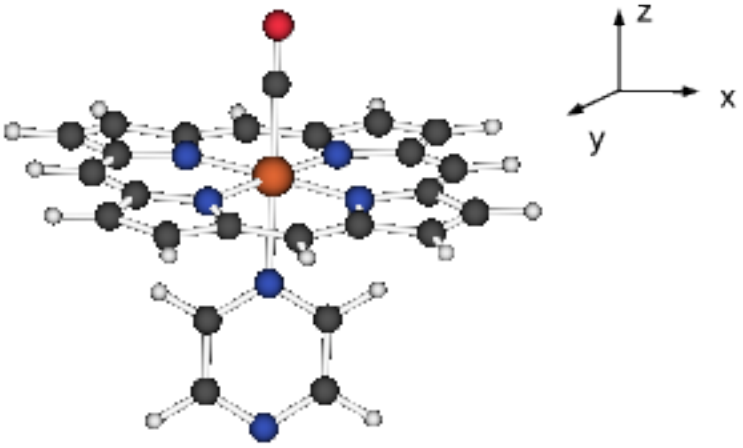

Figure 1: Iron center in a porphyrin (P), with CO and pyrazine (pz) as axial ligands (FeP(pz)CO)

The RASPT2 and CASPT2 calculations were carried out with the 7.8 MOLCAS package[36–38]. The Relativistic correlation-consistent Atomic Natural Orbitals basis sets used were the same as in Ref[31] (ANO-RCC basis sets[39]: Fe [7s6p5d2f1g]; C, N, O [4s3p1d]; H [2s1p]) and Cholesky decomposition technique was used to reduce the number of integrals[40,41]. The number of roots in the state-average CASSCF and RASSCF calculations varied according to the symmetry. The description of the singlet states up to the Soret Band required 5 roots for the A_2 symmetry, 8 roots of the B_1 and B_2 symmetries, while excited states of

A_1 symmetry were obtained using either 3 (for the first and the second excited states) or 5 roots calculations (for the third and the fourth excited states). Transition energies were calculated considering an electronic ground state energy calculated with the same number of roots as for the excited states. Core electrons were frozen except the 3s and 3p electrons of the iron atom which were correlated. A common level shift value of 0.4 a.u. was used for all the calculations. The calculations were performed with standard IPEA value of 0.25 a.u. and without IPEA shift. The oscillator strengths were calculated thanks to the restricted active space state interaction approach (RASSI)[42].

Choice of active spaces

The full set of valence π and π^* orbitals of the porphyrin together with the 3d-iron orbitals and the orbitals describing the metal-ligands interaction would constitute a 36 electrons in 36 orbitals active space. This exceeds by far the feasibility of CASSCF[43]. RASSCF is considered instead, which implies the partition of an active space in RAS1, RAS2 and RAS3 subspaces[44]. The validity of the partition must be checked with respect to the strongest correlation effects (possible strong covalent metal-ligand bonding effects and 3d double-shell effect in case of first-row transition metals) and to the orbitals becoming partially occupied through the electronic excitations[34]. We aim at describing the valence excited states until $\approx 3\ eV$ that means Metal Centered (MC) transitions ($d \rightarrow d$), Metal-to-Ligand-Charge-Transfer (MCLT) states ($d \rightarrow \pi^*$), Ligand-to-Metal-Charge-Transfer (LMCT) states ($\pi \rightarrow d$), and intra-porphyrin excitations ($\pi \rightarrow \pi^*$). We include in the RAS2 space, where all possible excitations are allowed, all the orbitals becoming singly occupied in at least one of the main determinants of these states, leading to a set of nine orbitals, namely the five $3d$ orbitals of the iron and the four Gouterman's orbitals which consist of the four frontier orbitals of the porphyrin ring (two occupied and two unoccupied). The orbitals of the RAS2 space obtained after an eight roots state averaged RASSCF for the A_1 symmetry, can be found in Figure 2, with their occupation in the electronic ground state. Further active orbitals are included in the RAS1 and RAS3 space where at most two holes and two particules are allowed. The composition of these spaces follows two goals : first the proper description of the iron and of the metal-ligand interaction and second a good description

of the π system of the porphyrin ring. The first goal is reached by including in the RAS1 space two metal-ligand σ-bonding orbitals, counterpart of the $3d$ ground state empty iron orbitals, and in the RAS3 space the three $3d'$ double shell orbitals correlating the three $3d$ ground state occupied orbitals. This leads to a 14 electrons in 14 orbitals active space, referred to as the small active space, matching the active space of the previous CASPT2 study[31]. A comparison of the RASPT2/CASPT2 results for this small active space enables the assessment of including the σ and $3d'$ orbitals only in a RAS1 or a RAS3 space, i.e. restricting the number of excitations from or into these orbitals. This will be discussed in the next subsection. Concerning the description of the porphyrin, due to the size of the RAS2 space, it is not possible to include all the remaining orbitals of the porphyrin π system. In practice, in addition to the four π orbitals of the RAS2 space, the 7 next highest occupied π orbitals are added to the RAS1 space and 5 virtual π^* orbitals are added to the RAS3 space, leading to a 28 electrons in 26 orbitals active space. This is equivalent to exclude the contribution of the β carbons of the pyrrole rings to the porphyrin π system, as has been done by Pierloot and coworkers[45]. The number of determinants in the total RASSCF space is about 35 millions of determinants. Plots of the RAS1 and RAS3 can also be found in Figure 2.

This 28e26a active space is already large and is designed to describe the metal center and the porphyrin π system. We do not include orbitals of the π system of the pyrazine group in the active spaces. Thus, electronic states involving excitations on the pyrazine ligand cannot be obtained by our calculations and are ignored in the present study. The (3s3p) correlation effect has been shown to be important in the spin state energetics of first-row transition metal complexes as discussed by Pierloot and collaborators[46,47]. In this work, we handle transition energies between states of same spin. The effect of (3s3p) correlation on the d-d transitions has been checked at the CASPT2 level, using a metallic-only active space, by including or not these orbitals in the active space. The results are presented in the supplementary material file (Table S2). The mean value of the differences on the transition energies with and without adding the 3s and 3p orbitals in the active space is of 0.1 and 0.06 eV without and with IPEA respectively. The effect is then small and only weakly dependent on the IPEA shift. These orbitals are not included in the RASSCF active space.

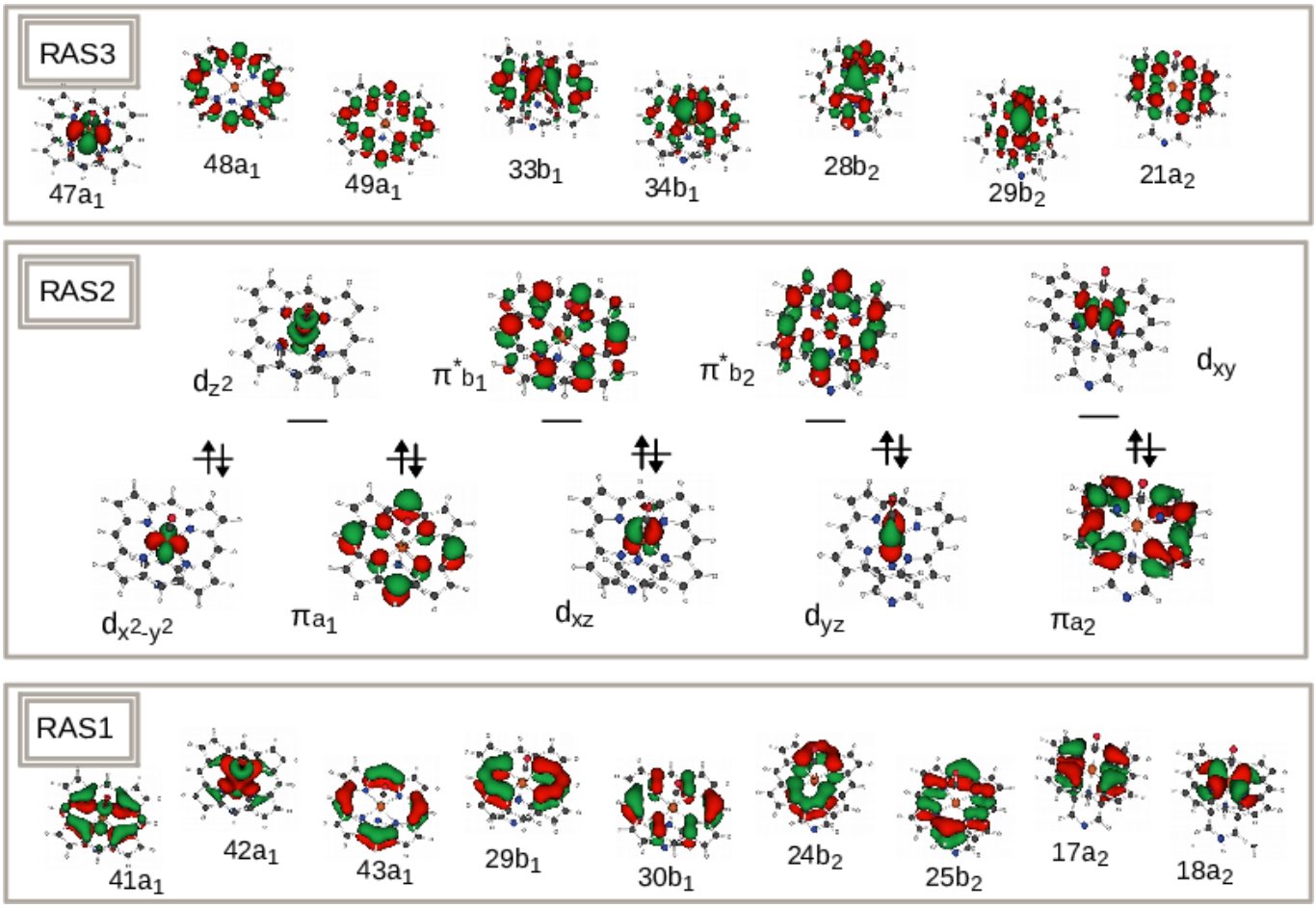

Figure 2: Active orbitals obtained after an eight roots state averaged RASSCF-28e26a calculation of A_1 symmetry for the FeP(pz)CO complex.

Comparison of CASPT2 and RASPT2 results for the 14e14a active space

The purpose of this subsection is to validate the transfer of some orbitals involved in the description of the metal or of the metal-ligand interaction from RAS2 to either RAS1 or RAS3 by comparing CASPT2 and RASPT2 results obtained with the same 14e14a active space. The electronic states issued from state-average CASSCF and RASSCF calculation can be clearly identified with the nature of the dominant configurations such as $d \rightarrow d$, $\pi \rightarrow \pi^*$ states etc... The detailed description of the electronic excited states of the targeted complex will be presented in the next section. Table S3 in the Supplementary Material gives

the difference between CASPT2-14e14a and RASPT2-14e14a calculation. The transition energies obtained at the RASPT2 level are systematically underestimated with respect to the CASPT2 ones, with a mean difference of 0.12 eV. Only two transition energies show a deviation larger than 0.16 eV, namely 0.37 and 0.38 eV. They correspond to the $d \rightarrow \pi^*$ states of B_1 and B_2 symmetries. In their respective symmetry, they are the only states with a d^5 configuration of the iron, the seven other states having a d^6 configuration. The orbitals, being optimized through a state-averaged procedure, might be less adapted to a d^5 configuration of the iron. A bias in the description of these two $d \rightarrow \pi^*$ states is thus possible and a restriction of possible excitations when going from CASSCF to RASSCF might further affect the transition energies. The difference is less important in case of the $d \rightarrow \pi^*$ states of A_1 and A_2 symmetries where 3-roots and 5-roots state-averaged calculations have been performed. In these cases, the deviations between the CASPT2-14e14a and the RASPT2-14e14a results range from 0.06 to 0.12 eV. For the $d \rightarrow d$ states which are directly concerned by the restriction of the excitations, the deviations are on average of 0.085 eV. As a conclusion, the inclusion of the σ orbitals in RAS1 and of the $3d'$ orbitals in RAS3, allowing at most double excitations out of or in these spaces, is a reasonable strategy leading, in the great majority of cases, to errors in the transition energies ranging from 0.02 to 0.16 eV.

RESULTS and DISCUSSION

Excited states of the iron-porphyrin-pyrazine-carbonyl complex

The transition energies, the oscillator strengths together with the electronic nature of the excited states of the FeP(pz)CO complex obtained from the RASPT2-28e26a calculation, without and with standard IPEA shift, are presented in Table 1. The different states are labelled and listed in the increasing energy order issued from the calculation without inclusion of the IPEA shift. We first discuss the electronic spectrum obtained without IPEA shift.

	Configurations	**Weights**	ΔE **(eV) (Osc. str.)** IPEA = 0.0 a.u.	ΔE **(eV)** IPEA = 0.25 a.u
a^1B_2	$d_{x^2-y^2} \rightarrow \pi^*_{b_2}$	0.55	1.76 (0.0021)	2.10
a^1B_1	$d_{x^2-y^2} \rightarrow \pi^*_{b_1}$	0.54	1.77 (0.0021)	2.11
a^1A_2	$d_{x^2-y^2} \rightarrow d_{xy}$	0.70	1.83 (0.0000)	1.98
b^1A_1	$d_{xz} \rightarrow \pi^*_{b_1}$	0.35	1.90 ($0.6\ 10^{-5}$)	2.36
	$d_{yz} \rightarrow \pi^*_{b_2}$	0.32		
b^1A_2	$d_{yz} \rightarrow \pi^*_{b_1}$	0.58	2.08 (0.0000)	2.40
c^1A_2	$d_{xz} \rightarrow \pi^*_{b_2}$	0.56	2.10 (0.0000)	2.44
c^1A_1	$d_{yz} \rightarrow \pi^*_{b_2}$	0.30	2.21 ($0.7\ 10^{-5}$)	2.68
	$d_{xz} \rightarrow \pi^*_{b_1}$	0.27		
b^1B_2	$d_{yz} \rightarrow d_{z^2}$	0.56	2.22 (0.0008)	2.48
	$d_{xz} \rightarrow d_{xy}$	0.18		
b^1B_1	$d_{xz} \rightarrow d_{z^2}$	0.56	2.22 (0.0001)	2.47
	$d_{yz} \rightarrow d_{xy}$	0.18		
c^1B_2	$\pi_{a_2} \rightarrow \pi^*_{b_1}$	0.39	2.30 (0.0154)	2.77
	$\pi_{a_1} \rightarrow \pi^*_{b_2}$	0.34		
c^1B_1	$\pi_{a_2} \rightarrow \pi^*_{b_2}$	0.39	2.31 (0.0118)	2.77
	$\pi_{a_1} \rightarrow \pi^*_{b_1}$	0.34		
d^1A_2	$\pi_{a_2} \rightarrow d_{z^2}$	0.31	2.61 (0.0000)	3.10
	$d_{yz}\ \pi_{a_2} \rightarrow d_{z^2}\ \pi^*_{b_2}$	0.19		
	$d_{xz}\ \pi_{a_2} \rightarrow d_{z^2}\ \pi^*_{b_1}$	0.20		
e^1A_2	$\pi_{a_1} \rightarrow d_{xy}$	0.32	2.67 (0.0000)	3.16
	$d_{yz}\ \pi_{a_1} \rightarrow d_{xy}\ \pi^*_{b_2}$	0.12		
	$d_{xz}\ \pi_{a_1} \rightarrow d_{xy}\ \pi^*_{b_1}$	0.11		

Table 1: **RASPT2(28e26a).** Transition energies of the FeP(pz)CO complex, together with the oscillator strengths and the configurations with weights larger than 0.10, calculated at the RASPT2 level with the 28e26a active space, with values of IPEA shift of 0. and 0.25 a.u. The excited states are labelled in the increasing energy order obtained without IPEA shift.

	Configurations	**Weights**	ΔE **(eV)** (***Osc. str.***) IPEA = 0.0 a.u.	ΔE **(eV)** IPEA = 0.25 a.u
d^1A_1	$d_{x^2-y^2} \rightarrow d_{z^2}$	0.43	2.74 (0.2 10^{-5})	3.12
e^1A_1	$\pi_{a_2} \rightarrow d_{xy}$	0.32	2.74 (0.3 10^{-5})	3.27
	$d_{yz}\ \pi_{a_2} \rightarrow d_{xy}\ \pi^*_{b_2}$	0.12		
	$d_{xz}\ \pi_{a_2} \rightarrow d_{xy}\ \pi^*_{b_1}$	0.13		
d^1B_2	$d_{x^2-y^2}\ \pi_{a_1} \rightarrow d_{xy}\ \pi^*_{b_1}$	0.67	2.84 (0.9 10^{-4})	3.33
d^1B_1	$d_{x^2-y^2}\ \pi_{a_1} \rightarrow d_{xy}\ \pi^*_{b_2}$	0.65	2.86 (0.0001)	3.36
e^1B_1	$d_{x^2-y^2}\ \pi_{a_2} \rightarrow d_{xy}\ \pi^*_{b_1}$	0.61	2.90 (0.0003)	3.44
f^1B_1	$\pi_{a_1} \rightarrow \pi^*_{b_1}$	0.36	2.93 (1.1898)	3.57
	$\pi_{a_2} \rightarrow \pi^*_{b_2}$	0.30		
e^1B_2	$d_{x^2-y^2}\ \pi_{a_2} \rightarrow d_{xy}\ \pi^*_{b_2}$	0.66	2.97 (0.1 10^{-4})	3.50
f^1B_2	$\pi_{a_1} \rightarrow \pi^*_{b_2}$	0.36	2.98 (1.2049)	3.62
	$\pi_{a_2} \rightarrow \pi^*_{b_1}$	0.29		
g^1B_1	$d_{yz} \rightarrow d_{xy}$	0.48	3.05 (0.0011)	3.38
	$d_{xz} \rightarrow d_{z^2}$	0.13		
g^1B_2	$d_{xz} \rightarrow d_{xy}$	0.48	3.06 (0.0008)	3.39
	$d_{yz} \rightarrow d_{z^2}$	0.13		
h^1B_2	$d_{x^2-y^2}\ \pi_{a_2} \rightarrow d_{z^2}\ \pi^*_{b_1}$	0.70	3.55 (0.0111)	4.06
h^1B_1	$d_{x^2-y^2}\ \pi_{a_2} \rightarrow d_{z^2}\ \pi^*_{b_2}$	0.70	3.58 (0.0076)	4.09

Table 1: **RASPT2(28e26a).**Continued.

The effect of IPEA and the effect of limiting the active space on the porphyrin ring will be discussed in the next subsections. The spectrum of the excited states is rather dense, with 23 excited states whose transition energies range from 1.76 eV to 3.06 eV. The most strongly absorbing states are two nearly degenerated excited states with transition energies of 2.93 eV (f^1B_1 state) and 2.98 eV (f^1B_2 state) respectively. They correspond to the second intraporphyrin $\pi \rightarrow \pi^*$ absorption band, referred to as the Soret Band in the literature. The second most strongly absorbing states correspond to the first $\pi \rightarrow \pi^*$ absorption band (the so-called Q band) at 2.30 eV (c^1B_2 state) and 2.31 eV (c^1B_1 state). The absorption intensity of the Q band is around 100 time weaker than that of the Soret Band. The closest available experimental data is the absorption spectrum of carboxyhemoglobin[48], a protein whose active site consists in a FeP(im)CO unit (im=imidazole). The strong Soret band has a maximum reported at 2.96 eV, while the Q band has two maxima of nearly same intensity at 2.18 eV and 2.30 eV[48]. Our theoretical results are thus very close to these experimental data, excepting the splitting of the Q band. This splitting could be due to the environmental effect of the protein, which tilts slightly the Fe-CO bond with respect to the porphyrin normal plan[49]. For the closely related FeP(im)CO complex in the gas phase, a TD-DFT study[13] based on the B3LYP functional reports $\pi \rightarrow \pi^*$ transitions at 2.40/2.42 eV for the Q band and 3.35/3.36 eV for the Soret band.

The oscillator strengths of the other types of excited states are smaller as can be seen in Table 1. The first MC transition appears at 1.83 eV (a^1A_2 state) and corresponds to an excitation from $d_{x^2-y^2}$ to d_{xy} , both orbitals being oriented in the porphyrin plane. The next MC transitions, at 2.22 eV (b^1B_1 and b^1B_2 states) correspond mainly to transitions into the d_{z^2} orbital which has an iron-CO antibonding character. This finding is thus consistent with the experimental observation of the photolysis of the carbonyl ligand from the heme after irradiation at 570 nm (2.18 eV)[5]. The MLCT states, involving excitations from a d orbital to an unoccupied Gouterman π^* orbital are located in the lowest part of the spectrum. The transition energies of the six states range from 1.76 to 2.21 eV. MLCT states involving charge transfer to the CO are not investigated here. In the previous CASPT2 study[31], with the appropriate active space, a first $d \rightarrow \pi^*_{CO}$ state was found at about 4.0 eV. Pure doubly excited states are found starting from 2.8 eV. They result from simultaneous mono-

excitations on both the iron center and the porphyrin ring. The lowest of these states are located about 2.8-3.0 eV above the electronic ground state in the vicinity of the Soret states. They are based on the first MC transition ($d_{x^2-y^2} \rightarrow d_{xy}$). The occurrence of such rather low-lying doubly excited states among the valence excited states comes from the large conjugated π system of the porphyrin ligand which results in a small HOMO-LUMO intra-ligand gap and could be specific to partially filled d-shell metalloporphyrins. Two other doubly excited states are reported at energies above 3.0 eV. Another group of states, characterised by a mixed character of LMCT ($\pi \rightarrow d$) and mixed double excitations, can be found around 2.70 eV.

Effect of the enlargement of the active space on the porphyrin ligand beyond the Gouterman's set

In this subsection we discuss the effect of extending the active space on the porphyrin beyond the four Gouterman orbitals. Investigations based on a DFT/MRCI treatment have concluded to the necessity to go beyond the Gouterman four-orbitals picture for the description of the Soret band, especially for the free-base porphyrin[50]. We present in Table 2 the transition energies obtained for the FeP(pz)CO complex at the CASPT2 level with the 14e14a active space. The signed differences between the RASPT2-28e26a and the CASPT2-14e14a transition energies without IPEA shift are reported in Table S4 of the Supplementary Material. The weights of the main configurations are similar in the RASSCF and CASSCF calculations, allowing for such a comparison. These differences in transition energies are small for the MC states with a mean unsigned difference of 0.14 eV. This is only slightly larger than the mean difference of 0.085 eV observed when comparing CASPT2-14e14a and RASPT2-14e14a, showing that, as expected, for d-d transitions, the inclusion of only the Gouterman set in the active space is sufficient. The inclusion of 12 additional orbitals of the π system in either the RAS1 or the RAS3 space has a larger but still moderate effect

	Configurations	**Weights**	ΔE **(eV) (Osc. str.)** IPEA = 0.0 a.u.	ΔE **(eV)** IPEA = 0.25 a.u
a^1B_1	$d_{x^2-y^2} \rightarrow \pi^*_{b_1}$	0.68	1.48 (0.0028)	1.99
a^1B_2	$d_{x^2-y^2} \rightarrow \pi^*_{b_2}$	0.69	1.50 (0.0027)	2.01
c^1B_1	$\pi_{a_2} \rightarrow \pi^*_{b_2}$	0.50	1.69 (0.0248)	2.69
	$\pi_{a_1} \rightarrow \pi^*_{b_1}$	0.37		
c^1B_2	$\pi_{a_2} \rightarrow \pi^*_{b_1}$	0.51	1.71 (0.0308)	2.71
	$\pi_{a_1} \rightarrow \pi^*_{b_2}$	0.37		
b^1A_1	$d_{xz} \rightarrow \pi^*_{b_1}$	0.42	1.75 ($0.7\ 10^{-2}$)	2.42
	$d_{yz} \rightarrow \pi^*_{b_2}$	0.41		
b^1A_2	$d_{yz} \rightarrow \pi^*_{b_1}$	0.74	1.93 (0.0000)	2.38
a^1A_2	$d_{x^2-y^2} \rightarrow d_{xy}$	0.83	1.95 (0.0000)	2.13
c^1A_2	$d_{xz} \rightarrow \pi^*_{b_2}$	0.74	1.95 (0.0000)	2.41
c^1A_1	$d_{yz} \rightarrow \pi^*_{b_2}$	0.39	1.99 (0.0011)	2.64
	$d_{xz} \rightarrow \pi^*_{b_1}$	0.28		
d^1B_2	$d_{x^2-y^2}\ \pi_{a_1} \rightarrow d_{xy}\ \pi^*_{b_1}$	0.79	2.29 (0.0001)	3.29
d^1B_1	$d_{x^2-y^2}\ \pi_{a_1} \rightarrow d_{xy}\ \pi^*_{b_2}$	0.80	2.31 (0.0001)	3.30
b^1B_2	$d_{yz} \rightarrow d_{z^2}$	0.64	2.36 (0.0001)	2.63
	$d_{xz} \rightarrow d_{xy}$	0.22		
b^1B_1	$d_{xz} \rightarrow d_{z^2}$	0.64	2.36 (0.0001)	2.63
	$d_{yz} \rightarrow d_{xy}$	0.22		
e^1A_2	$\pi_{a_1} \rightarrow d_{xy}$	0.21	2.49 (0.0000)	3.69
	$d_{yz}\ \pi_{a_1} \rightarrow d_{xy}\ \pi^*_{b_2}$	0.12		
	$d_{xz}\ \pi_{a_1} \rightarrow d_{xy}\ \pi^*_{b_1}$	0.12		

Table 2: **CASPT2(14e14a).** Transition energies of the FeP(pz)CO complex, together with the oscillator strengths and the configurations with weights larger than 0.10, calculated at the CASPT2 level with the 14e14a active space, with values of IPEA shift of 0. and 0.25 a.u. The excited states are listed in the increasing energy order obtained without IPEA shift. Their labels correspond to those attributed following to the RASPT2-28e26a calculation.

	Configurations	**Weights**	ΔE **(eV)** IPEA = 0.0 a.u.	ΔE **(eV)** IPEA = 0.25 a.u
d^1A_2	$\pi_{a_2} \rightarrow d_{z^2}$	0.27	2.50 (0.0000)	3.40
	$d_{yz}\ \pi_{a_2} \rightarrow d_{z^2}\ \pi^*_{b_2}$	0.26		
	$d_{xz}\ \pi_{a_2} \rightarrow d_{z^2}\ \pi^*_{b_1}$	0.28		
f^1B_1	$\pi_{a_1} \rightarrow \pi^*_{b_1}$	0.48	2.63 (1.2881)	3.78
	$\pi_{a_2} \rightarrow \pi^*_{b_2}$	0.34		
e^1B_1	$d_{x^2-y^2}\ \pi_{a_2} \rightarrow d_{xy}\ \pi^*_{b_1}$	0.80	2.67 (0.0000)	3.58
f^1B_2	$\pi_{a_1} \rightarrow \pi^*_{b_2}$	0.48	2.68 (1.2982)	3.82
	$\pi_{a_2} \rightarrow \pi^*_{b_1}$	0.34		
e^1A_1	$\pi_{a_2} \rightarrow d_{xy}$	0.19	2.69 ($0.6\ 10^{-6}$)	3.65
	$d_{yz}\ \pi_{a_2} \rightarrow d_{xy}\ \pi^*_{b_2}$	0.19		
	$d_{xz}\ \pi_{a_2} \rightarrow d_{xy}\ \pi^*_{b_1}$	0.21		
e^1B_2	$d_{x^2-y^2}\ \pi_{a_2} \rightarrow d_{xy}\ \pi^*_{b_2}$	0.79	2.71 (0.0000)	3.62
d^1A_1	$d_{x^2-y^2} \rightarrow d_{z^2}$	0.71	2.88 ($0.2\ 10^{-5}$)	3.23
g^1B_1	$d_{yz} \rightarrow d_{xy}$	0.57	3.19 (0.0001)	3.54
	$d_{xz} \rightarrow d_{z^2}$	0.17		
g^1B_2	$d_{xz} \rightarrow d_{xy}$	0.57	3.21 (0.0008)	3.55
	$d_{yz} \rightarrow d_{z^2}$	0.17		
h^1B_2	$d_{x^2-y^2}\ \pi_{a_2} \rightarrow d_{z^2}\ \pi^*_{b_1}$	0.80	3.33 (0.0103)	4.23
h^1B_1	$d_{x^2-y^2}\ \pi_{a_2} \rightarrow d_{z^2}\ \pi^*_{b_2}$	0.80	3.38 (0.0011)	4.27

Table 2: **CASPT2(14e14a).** Continued.

on the MLCT states: 0.20 eV on average, with a maximum of 0.29 eV. The largest effect is observed for the two states corresponding to the Q band namely the first intraporphyrin excited states c^1B_1 and c^1B_2, for which the extension of the active space increases the transition energies from 1.69 eV to 2.31 eV and 1.71 eV to 2.30 eV respectively. Thus for the Q band, the extension of the active space significantly improves the agreement with experiment (2.18-2.30 eV). The effect on the Soret band is limited to 0.30 eV but the agreement with experiment is also improved by the enlargement. Three orbitals can be distinguished among the porphyrin π system, in addition to the Gouterman orbitals, as playing a role at the non-dynamical correlation level. The $30b_1$ and $25b_2$ orbitals of the RAS1 space and the $48a_1$ orbital of the RAS3 space (see Figure 2) are singly occupied in several determinants with weights of the order of 0.5 to 1% in the wavefunction development of the Q and Soret states. For pure doubly excited states, the enlargement of the active space increases the transition energies of an amount of 0.20 to 0.55 eV. Concerning LMCT-doubly excited states, the effect is moderate, at most of 0.18 eV.

Effect of IPEA shift

The effect of inclusion of the IPEA shift in the RASPT2-28e26a can be analysed from Table 1 and from Table S5 (Supplementary Material) which reports the difference between transition energies computed with and without IPEA shift, for all the excited states sorted by electronic character and symmetry. The smallest effect is seen on the d-d transition energies with a mean difference of 0.28 eV, while the effect is a little bit larger for the MLCT states (0.38 eV on average). These increases of transition energies are similar to those reported in the original publication introducing the IPEA shift[23], where values ranging from about 0.2 to 0.4 eV are reported about tests on the N_2 and the benzene molecules. For the other types of states, which involve intraporphyrin excitations or at least depopulation of a porphyrin π orbital, mean values of the increases range from 0.46 to 0.64 eV. Due to the high density of excited states, the introduction of the IPEA shift changes some relative positions of the different excited states. Some relative orders of the lowest d-d states and the MLCT states are modifed, but in both cases, with or without IPEA shift, the MLCT states lie below the Q absorption band of the porphyrin. Another feature persisting after the introduction of

	ΔE (eV)				
	RASPT2-28e26a		CASPT2-14e14a		Exp.[48]
	IPEA=0.0 a.u.	IPEA=0.25 a.u.	IPEA=0.0 a.u.	IPEA=0.25 a.u	
Q band	2.30	2.77	1.71	2.71	2.18 , 2.30
	2.31	2.77	1.69	2.69	
Soret	2.93	3.57	2.63	3.78	2.96
band	2.98	3.62	2.68	3.82	

Table 3: Transition energies of the excited states corresponding to the Q Band and the Soret Band, obtained from RASPT2 (28e28a active space) and CASPT2 (14e14a active space) calculations with IPEA=0.0 a.u. and IPEA=0.25 a.u.. Experimental results corresponding to the absorption spectra of carboxyhemoglobin is also reported[48].

IPEA shift is the fact that some doubly excited states, based on the lowest d-d transition, are nearly degenerated with the intraporphyrin excitations forming the strongly absorbing Soret band. Also, the states with Ligand-to-Metal-Charge-Transfer ($\pi \rightarrow d$) character lie below the Soret band.

The effect of the inclusion of the IPEA in the CASPT2-14e14a calculation, where the active orbitals on the porphyrin ligand are limited to the Gouterman's set, is pointed out in Table S6 of the Supplementary Material. The effect on the d-d states is nearly identical to the one observed for the large active space (0.29 eV on average) but the introduction of the IPEA shift increases the transition energies of states involving intraporphyrin excitation of about 1 eV. This very large effect of IPEA on the transition energies of theses states with a 14e14a active space was already emphasized in our previous work[31]. The present calculation shows that the inclusion of π orbitals of the porphyrin ring beyond the Gouterman's set in the active space significantly reduces the effect of the IPEA shift (from about 1 eV to 0.5 eV) and keeps the effect in more usual values.

In Table 3 are collected together the RASPT2-28e26a and CASPT2-14e14a transition energies without and with IPEA, for the Q band and the Soret band together with the

nearest available experimental results[48]. The small difference between the RASPT2-28e26a and CASPT2-14e14a results obtained with the standard IPEA suggests that the truncation of the active space is hidden by the use of the IPEA shift. The RASPT2 results for the Q band and the Soret band are very close to the experimental results as long as the IPEA shift is omitted. Inclusion of standard IPEA in the RASPT2 deteriorates this good agreement. This finding corroborates the conclusion of the RASPT2 calculations of Kerridge[28] on regular metalloporphyrins with either magnesium or zinc as central atom. In this work, where the entire π orbitals system was included in the active space, experimental transition energies were best reproduced by RASPT2 calculations without inclusion of IPEA shift[28]. More generally, a recent work about the use of IPEA on the transition energies of organic systems has concluded that the introduction of IPEA was in fact not needed[24]. Our work points out that the dependence of the transition energies on the IPEA should be further investigated and particularly in case of large effects. A connection with a possible truncation of the active space should than be investigated.

CONCLUSIONS

Calculations of the singlet valence excited states of an iron-porphyrin-pyrazine-carbonyl complex up to the Soret band (about 3 eV) are presented. This complex has at the same time an organic chromophore and a metallic center absorbing both in the same energy range. The investigations are performed at the RASPT2 level involving an extended active space on the porphyrin ligand (16 π orbitals) in addition to the 10 active orbitals needed for the description of the metal-ligands interactions, leading to a total active space of 28 electrons in 26 orbitals. The variety of excited states to be considered (charge transfer states, metal centered and intraporphyrin excitations) leads to a RAS2 space of 9 orbitals. MLCT states $d \rightarrow \pi^*$ and some MC $d \rightarrow d$ transitions are found in the lowest part of the spectra, below the first $\pi \rightarrow \pi^*$ intraporphyrin transitions (Q band). Doubly excited states involving simultaneous intraporphyrin and metal-centered excitations, together with porphyrin-to-metal contributions, are found in the vicinity of the second intraporphyrin excitations, namely the strongly

absorbing Soret band. The extension of the active space on the porphyrin ligand beyond the Gouterman's orbitals is seen to have a strong effect on the states involving intraporphyrin excitations. First, the transition energies of the Q band are significantly improved. Secondly, the effect of inclusion of the IPEA shift on the transition energies is divided by a factor two. The best agreement with the closest available experimental results on the intraporphyrin excitations is obtained without the inclusion of the IPEA shift and the introduction of the IPEA shift deteriorates this agreement. We conclude from the present work, concerning only singlet valence states, that the IPEA shift should be used carefully and that transitions energies with and without IPEA should be compared.

References

1. X. Huang and J. T. Groves, Chem. Rev. **118**, 2491 (2018).
2. R. A. Baglia, J. P. T. Zaragoza, and D. P. Goldberg, Chem. Rev. **117**, 13320 (2017).
3. M. M. Pereira, L. D. Dias, and M. J. F. Calvete, ACS Catalysis **8**, 10784 (2018).
4. J. W. Petrich, C. Poyart, and J. L. Martin, Biochemistry **27**, 4049 (1988).
5. S. Franzen, L. Kiger, C. Poyart, and J.-L. Martin, Biophys. J. **80**, 2372 (2001).
6. A. S. Rury, T. E. Wiley, and R. J. Sension, Acc. Chem. Res. **48**, 860 (2015).
7. M.-H. Ha-Thi, N. Shafizadeh, L. Poisson, and B. Soep, J. Phys. Chem. A **117**, 8111 (2013).
8. T. Polack, J. P. Ogilvie, S. Franzen, M. H. Vos, M. Joffre, J.-L. Martin, and A. Alexandrou, Phys. Rev. Lett. **93** (2004).
9. J. Treuffet, K. J. Kubarych, J.-C. Lambry, E. Pilet, J.-B. Masson, J.-L. Martin, M. H. Vos, M. Joffre, and A. Alexandrou, Proc. Natl. Acad. Sci. U. S. A. **104**, 15705 (2007).
10. P. Nuernberger, K. F. Lee, A. Bonvalet, M. H. Vos, and M. Joffre, J. Phys. Chem. Lett. **1**, 2077 (2010).
11. C. Ventalon, J. M. Fraser, M. H. Vos, A. Alexandrou, J.-L. Martin, and M. Joffre, Proc. Natl. Acad. Sci. U. S. A. **101**, 13216 (2004).
12. A. Dreuw, B. D. Dunietz, and M. Head-Gordon, J. Am. Chem. Soc. **124**, 12070 (2002).
13. B. D. Dunietz, A. Dreuw, and M. Head-Gordon, J. Phys. Chem. B **107**, 5623 (2003).
14. K. Falahati, H. Tamura, I. Burghardt, and M. Huix-Rotllant, Nat. Commun. **9**, 4502 (2018).
15. C. Meier and M.-C. Heitz, J. Chem. Phys. **123**, 044504 (2005).
16. C. Falvo, A. Debnath, and C. Meier, J. Chem. Phys. **138**, 145101 (2013).

17. P.-Å. Malmqvist, K. Pierloot, A. R. M. Shahi, C. J. Cramer, and L. Gagliardi, J. Chem. Phys. **128**, 204109 (2008).

18. K. Andersson, P.-Å. Malmqvist, B. O. Roos, A. J. Sadlej, and K. Wolinski, J. Phys. Chem. **94**, 5483 (1990).

19. M. Cerdonio, A. Congiu-Castellano, F. Mogno, B. Pispisa, G. L. Romani, and S. Vitale, Proceedings of the National Academy of Sciences **74**, 398 (1977).

20. N. Schuth, S. Mebs, D. Huwald, P. Wrzolek, M. Schwalbe, A. Hemschemeier, and M. Haumann, Proceedings of the National Academy of Sciences **114**, 8556 (2017).

21. H. Chen, W. Lai, and S. Shaik, The Journal of Physical Chemistry B **115**, 1727 (2011).

22. H. Lischka, D. Nachtigallová, A. J. A. Aquino, P. G. Szalay, F. Plasser, F. B. C. Machado, and M. Barbatti, Chem. Rev. **118**, 7293 (2018).

23. G. Ghigo, B. O. Roos, and P. Åke Malmqvist, Chem. Phys. Lett. **396**, 142 (2004).

24. J. P. Zobel, J. J. Nogueira, and L. Gonzalez, Chem. Sci. **8**, 1482 (2017).

25. Wolaáski, D. Grabarek, and T. Andruniów, J. Comput. Chem. **39**, 1470 (2018).

26. S. Vela, M. Fumanal, J. Ribas-Ariño, and V. Robert, J Comput Chem **37**, 947 (2016).

27. M. Kepenekian, V. Robert, and B. Le Guennic, J. Chem. Phys. **131**, 114702 (2009).

28. A. Kerridge, Phys. Chem. Chem. Phys. **15**, 2197 (2013).

29. M. Gouterman, J. Chem. Phys. **30**, 1139 (1959).

30. M. Gouterman, J. Mol. Spectrosc. **6**, 138 (1961).

31. N. Ben Amor, A. Soupart, and M.-C. Heitz, J. Mol. Model. **23**, 53 (2017).

32. G. Alcover-Fortuny, R. Caballol, K. Pierloot, and C. de Graaf, Inorg. Chem. **55**, 5274 (2016).

33. A. L. B. Formiga, S. Vancoillie, and K. Pierloot, Inorg. Chem. **52**, 10653 (2013).

34. S. Vancoillie, H. Zhao, V. T. Tran, M. F. A. Hendrickx, and K. Pierloot, J. Chem. Theory Comput. **7**, 3961 (2011).

35. B. M. Bode and M. S. Gordon, J. Mol. Graphics Modell. **16**, 133 (1998).

36. F. Aquilante, L. De Vico, N. Ferré, G. Ghigo, P.-Å. Malmqvist, P. Neogrády, T. B. Pedersen, M. Pitoňák, M. Reiher, B. O. Roos, et al., J. Comput. Chem. **31**, 224 (2010).

37. V. Veryazov, P.-O. Widmark, L. Serrano-Andrés, R. Lindh, and B. O. Roos, Int. J. Quantum Chem. **100**, 626 (2004).

38. G. Karlström, R. Lindh, P.-Å. Malmqvist, B. O. Roos, U. Ryde, V. Veryazov, P.-O. Widmark, M. Cossi, B. Schimmelpfennig, P. Neogrady, et al., Comput. Mat. Science **28**, 222 (2003).

39. B. O. Roos, R. Lindh, P.-Å. Malmqvist, V. Veryazov, and P.-O. Widmark, J. Phys. Chem. A **108**, 2851 (2004).

40. F. Aquilante, T. B. Pedersen, and R. Lindh, J. Chem. Phys. **126**, 194106 (2007).

41. F. Aquilante, P.-Å. Malmqvist, T. B. Pedersen, A. Ghosh, and B. O. Roos, J. Chem. Theory Comput. **4**, 694 (2008).

42. P.-Å. Malmqvist, B. O. Roos, and B. Schimmelpfennig, Chem. Phys. Lett. **357**, 230 (2002).

43. B. O. Roos, P. R. Taylor, and P. E. Siegbahn, Chem. Phys. **48**, 157 (1980).

44. V. Sauri, L. Serrano-Andrés, A. R. M. Shahi, L. Gagliardi, S. Vancoillie, and K. Pierloot, J. Chem. Theory Comput. **7**, 153 (2011).

45. M. Radoń, E. Broclawik, and K. Pierloot, J. Chem. Theory Comput. **7**, 898 (2011).

46. K. Pierloot, Q. M. Phung, and A. Domingo, J. Chem. Theory Comput. **13**, 537 (2017).

47. Q. M. Phung, M. Feldt, J. N. Harvey, and K. Pierloot, J. Chem. Theory Comput. **14**, 2446 (2018).

48. M. W. Makinen and W. A. Eaton, Ann. N. Y. Acad. Sci. **206**, 210 (1973).

49. S. D. Longa, A. Arcovito, M. Girasole, J. L. Hazemann, and M. Benfatto, Phys. Rev. Lett. **87**, 155501 (2001).

50. A. Parusel and S. Grimme, Journal of Porphyrins and Phthalocyanines **5**, 225 (2001).